Z. Phys. Chem. **222** (2008) 1389–1406 / **DOI** 10.1524/zpch.2008.5401

DFT Calculations of ^{51}V Solid-State NMR Parameters of Vanadium(V) Model Complexes

By Torsten Gutmann[1], Annika Schweitzer[1], Maria Wächtler[1], Hergen Breitzke[1], Axel Buchholz[2], Winfried Plass[2], and Gerd Buntkowsky[2,*]

[1] Institut für Physikalische Chemie, Friedrich-Schiller-Universität Jena, Helmholtzweg 4, D-07743 Jena, Germany
[2] Institut für Anorganische und Analytische Chemie, Carl-Zeiss-Promenade 10, D-07745 Jena, Germany

Dedicated to Prof. Dr. Hans-Heinrich Limbach on the occasion of his 65th birthday

(Received March 20, 2008; accepted May 29, 2008)

Solid-State NMR / Vanadium / Haloperoxidase / DFT / Quadrupolar Interaction / Chemical Shift Anisotropy

Two *cis*-dioxovanadium(V) complexes and three monooxovanadium(V) complexes with different coordination numbers and ligand spheres, serving as model complexes for vanadium haloperoxidases, were studied by ^{51}V solid-state NMR spectroscopy. The most important ^{51}V solid-state NMR parameters (quadrupolar coupling constant C_Q, asymmetry of the EFG tensor η_Q, isotropic chemical shift δ_{iso}, chemical shift anisotropy δ_σ, asymmetry of the CSA tensor η_σ and the Euler angles α, β and γ) describing the quadrupolar and chemical shift anisotropy interactions were determined theoretically with DFT methods employing the B3LYP functional and experimentally using genetic fitting algorithms. Calculations of δ_{iso} values were treated with different referencing values of $VOCl_3$ computed with different-sized basis sets using the "counterpoise method". The calculated C_Q values were discussed in terms of the quadrupolar moment Q. Absolute tensor orientations of CSA and EFG tensors were computed by DFT. These orientations were found to correlate to structural features of the model complexes.

1. Introduction

Vanadium occurs naturally in various minerals as for example in galena (vanadinite), patronite or carnotite [1]. Furthermore, it functions as co-factor in the active site of several haloperoxidases [2–5] which catalyze the oxidation of hal-

* Corresponding author. E-mail: mailto:gerd.buntkowsky@uni-jena.de

ides to hypohalous acid (Eq. 1). Hypohalous acid is capable to halogenate natural organic substrates [6–8] or in absence of an appropriate substrate to generate singlet-oxygen [9].

$$H_2O_2 + X^- + H^+ \rightarrow H_2O + HOX \quad (1)$$

The detailed investigation of the catalytic processes in the course of this reaction is a matter of current interest [10–18]. To solve this problem a whole range of vanadium model complexes which are intended to mimic the structure and function of the active site of haloperoxidases have been reported [19–22]. Moreover, the design of efficient enzyme mimics is a desirable goal, as this can lead to new methods and pathways in organic synthesis [23, 24].

The abundant vanadium isotope ^{51}V (99.75%) is a quadrupolar nucleus with a nuclear spin of $I = 7/2$. It can be studied by liquid-state and solid-state NMR spectroscopy [25–34]. The main interest in the solid-state NMR experiments is the determination of the ^{51}V NMR parameters, namely the chemical shift anisotropy (CSA) tensor and the electric field gradient (EFG) tensor. In general these parameters dominate the spectrum. They reflect the molecular and electronic structure in the vicinity of the ^{51}V nucleus. Their determination is therefore the first step in understanding the structural features in the vicinity of the vanadium atom. This can be done on two different levels, namely on the experimental level and/or on the quantum chemical level. In the latter these parameters are calculated by quantum chemical techniques [29, 30, 35–41]. The final step is the interpretation of these data in terms of structural properties. For this step appropriate correlations still have to be developed. Moreover, one has to deal with the problem that a solid base on the quantum chemical level is not developed up to now. In particular one faces the problem that the referencing of the calculated chemical shift values in the case of ^{51}V is still not sufficiently well established. In many calculations the isotropic chemical shift values δ_{iso} are extremely overestimated, if DFT methods employing the B3LYP functional with specific basis sets like 6–311+G and TZV [29] or 6–311G(d) [30] are employed for calculations.

Different methods can be employed for the referencing of the chemical shift to a standard [42] : If the chemical shift is solely determined from DFT calculations without using any experimental data for referencing, the calculation of both, the system of interest and the referencing system is necessary. In the case of ^{51}V solid-state NMR spectroscopy the common reference system is $VOCl_3$, a relatively small molecule, which however differs strongly from the systems of interest. This causes a problem in the referencing, since two different sized molecular systems (number of atoms: $N = 5$ for $VOCl_3$; $N \geq 31$ for model complexes) have to be compared for the calculation of the relative isotropic chemical shift. If the same basis set is used for both calculations, the number of basis functions is significantly lower for the smaller molecule than for the model complex. The result is a lower accuracy of the calculated energy and thus of the absolute shielding of the small referencing molecule.

One possibility to handle this problem is the "counterpoise method" developed by Boys and Bernardi already in 1970 [43]. It determines a correction of energy by calculating the difference between the energy of the reference system calculated with the same basis set as the system of interest and the reference system calculated with additional basis functions from the system of interest. The latter are localized at atomic positions of the system of interest. These sets of basis functions are termed "ghost basis".

In our computations we apply this method to the calculation of the energy of the $VOCl_3$ to achieve a more accurate determination of its absolute shielding. For this, calculations with different sized "ghost basis" generated from the model complexes **Ia**-**Va** (Fig. 1) are employed.

The final result of the calculations are the main ^{51}V solid-state NMR parameters: isotropic chemical shifts δ_{iso}, asymmetry of the CSA tensors δ_σ and the quadrupolar coupling constants C_Q. As an experimental example five distinct vanadium(V) complexes with structural differences in the surrounding of the vanadium center are compared. In addition the orientation of the tensors in the molecular frame is discussed and some preliminary correlations between the orientation of CSA and EFG tensors at the vanadium center and the electronic structure of the model complexes are developed.

2. Theoretical section

2.1 Investigated model complexes

The five studied model complexes **I**-**V** are shown in Fig. 1. **I** and **II** are *cis*-dioxovanadium(V) compounds. They are based on a Schiff-base ligand derived salicylidene hydrazide with different functionalized side chains [44–46]. Complexes **I** and **II** are present as ammonium salt. This leads in both cases to an extended hydrogen bonding network in the solid-state structure, which contains an additional water molecule in **I** and a methanol molecule in **II**. The vanadium centers of **I** and **II** are located in a nearly square pyramidal surrounding.

Complexes **III**-**V** are monooxovanadium(V) compounds. In **IV** a trigonal bipyramidal geometry is found for the vanadium center and the ligand sphere includes an imine function [47]. In contrast to this the vanadium centers in complexes **III** and **V** are found in a distorted octahedral geometry. Complex **III** contains a mixed-ligand system with a salicylidene hydrazide ligand and a quinoline coligand [20]. The coordination sphere in complex **V** is formed by a five dentate amino alcohol ligand [48, 49].

2.2 General aspects of ^{51}V solid-state NMR parameters

^{51}V is a highly favorable nucleus for solid-state NMR studies. Main reasons are the high gyromagnetic ratio (Larmor frequency of 105.19 MHz at 9.4 T) and the

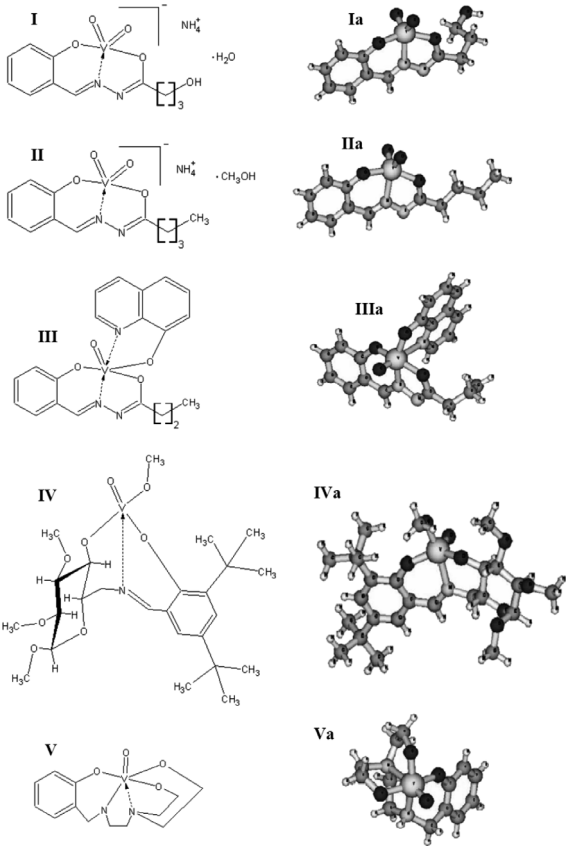

Fig. 1. Chemical structures of the model complexes **I**-**V** and corresponding 3D models **Ia**-**Va** cut from the X-ray structure of the model complexes **I**-**V**.

relatively small quadrupolar moment ($Q = -5.2 \cdot 10^{-30}$ m^2) [50, 51]. As a result of these properties, even small quantities of vanadium are easily detectable by NMR spectroscopy.

The total spin Hamiltonian (Eq. 2) of the vanadium nucleus may be expressed as a sum of individual Hamiltonians

$$H = H_{Zeeman} + H_{RF} + H_D + H_{CSA} + H_Q^{(1)} + H_Q^{(2)} \quad (2)$$

with H_{Zeeman} being the Zeeman interaction, H_{RF} the radio frequency field, H_D the dipolar interaction, H_{CSA} the chemical shift anisotropy interactions and $H_Q{}^{(1)}$ as well as $H_Q{}^{(2)}$ the quadrupolar interactions of first and second order.

The ^{51}V MAS NMR spectra are dominated by the last three terms. The five parameters characterizing the corresponding interaction tensors – isotropic chemical shift δ_{iso}, chemical shift anisotropy δ_σ, asymmetry of the CSA tensor

η_σ, quadrupolar coupling constant C_Q, asymmetry of the EFG tensor η_Q – are defined according to Eqs. 3 and 4

$$\delta_{iso} = \frac{\delta_{11} + \delta_{22} + \delta_{33}}{3}$$
$$\delta_\sigma = \delta_{33} - \delta_{iso} \quad \eta_\sigma = \frac{\delta_{22} - \delta_{11}}{\delta_{33} - \delta_{iso}} \tag{3}$$

$$C_Q = \frac{eQV_{zz}}{h} \quad \eta_Q = \frac{V_{xx} - V_{yy}}{V_{zz}} \tag{4}$$

where δ_{11}, δ_{22} and δ_{33} describe the eigenvalues of the symmetrized CSA tensor with

$$|\delta_{11} - \delta_{iso}| \leq |\delta_{22} - \delta_{iso}| \leq |\delta_{33} - \delta_{iso}|.$$

V_{xx}, V_{yy} and V_{zz} express the principal components of the EFG tensor with

$$|V_{xx}| \leq |V_{yy}| < |V_{zz}|.$$

Q defines the quadrupole moment of the nucleus, e the electronic charge and h the Planck constant.

For a full description of the system, six more parameters are necessary, namely two sets of Euler angles defining the orientation of these tensors in a molecular reference frame. As common in solid-state NMR the Euler angle definition of Rose [52] is chosen. Owing to the 180° symmetry of magnetic interactions, their choice is not unique. Employing the symmetry transformations given in Fernandez [53] all Euler angles were transformed into the standard range $\alpha \in [0°, 90°]$, $\beta \in [0°, 90°]$ and $\gamma \in [0°, 180°]$. From experiments on non-oriented powder samples however, only the relative orientations of the two tensors are obtainable, owing to the lack of an absolute reference frame. This relative orientation is described by the set of Euler angles α, β and γ. Thus in total eight parameters are necessary for a full description of an experimental spectrum. These parameters are in general obtained by stepwise fitting of the numerical simulated ^{51}V NMR spectrum to the experimental spectra [26–33] and can be compared to the results of quantum mechanical calculations of the CSA and EFG tensor on structural models using DFT methods [29, 30, 39, 41].

2.3 Computational details

DFT calculations were performed with the model structures **Ia**-**Va** shown in Fig. 1. These models represent fragments of the whole solid-state X-ray structures of the compounds **I**-**V**. The negatively charged structures **Ia** and **IIa** are models for the anions of compounds **I** and **II**. The neutral fragments **IIIa**-**Va** are models of the uncharged complexes **III**-**V**.

The solid-state NMR parameters describing the anisotropic properties of the ^{51}V interaction tensors (δ_σ, η_σ, C_Q and η_q) are extracted directly from the magnetic shielding tensor

Table 1. Absolute shielding values of $VOCl_3$ in ppm calculated with different sized "ghost basis" namely the "ghost basis" of the first ligand sphere of the model complexes **Ia**-**Va** (frag) and the "ghost basis" of the common ligand of the model complexes **Ia**-**Va** (comp).

	631G(d)	631++G(d, p)	6311G	6311+G	6311G(d)	TZV	TZVP
$VOCl_3$ without "ghost basis"	−1945.2	−1953.4	−2340.7	−2287.8	−2240.2	−2325.6	−2223.1
Ia frag	−1947.5	−1935.8	−2288.4	−2259.1	−2208.5	−2264.8	−2202.9
Ia comp	−1948.1	−1914.8	−2280.6	−2252.9	−2206.3	−2256.7	−2202.9
IIa frag	−1969.1	−1930.3	−2269.5	−2248.2	−2207.0	−2256.0	−2206.0
IIa comp	−1965.9	−1930.3	−2265.5	−2242.4	−2205.4	−2243.5	−2200.4
IIIa frag	−1932.8	−1939.3	−2281.4	−2261.7	−2204.9	−2278.8	−2205.2
IIIa comp	−1931.3	−1922.2	−2267.7	−2254.5	−2200.0	−2261.3	−2202.3
IVa frag	−1964.6	−1927.1	−2279.9	−2255.1	−2209.1	−2268.8	−2210.5
IVa comp	−1957.6	−1895.0	−2266.7	−2235.8	−2204.5	−2248.4	−2197.4
Va frag	−1966.0	−1940.8	−2259.9	−2240.9	−2202.3	−2240.7	−2196.0
Va comp	−1962.1	−1939.2	−2251.1	−2232.0	−2200.2	−2231.4	−2200.8

$$\tilde{\sigma} = \frac{\partial^2 E}{\partial B_0 \partial \mu_I}$$

and the components of the EFG tensor

$$V_{ij}^{(A)} = \int d^3 s \; \rho_e \frac{(3 s_{A,i} s_{A,j} - \delta_{ij} s_A^2)}{s_A^5}$$

at the vanadium center, calculated by the DFT methods. The isotropic chemical shift δ_{iso} of the complexes is calculated by referencing the absolute magnetic shielding σ_{iso} of the complex with respect to the absolute magnetic shielding of the external standard $VOCl_3$.

For the calculation of the absolute shielding values of $VOCl_3$ as reference, three different strategies were compared: (i) calculations employing the unmodified X-ray structure [54] of $VOCl_3$ using a basis set without additional basis functions of the molecules of interest; (ii) calculations employing the X-ray structure of $VOCl_3$ plus additional basis functions from the atoms of the first ligand sphere of the complexes **Ia**-**Va** as "ghost basis"; (iii) calculations employing the X-ray structure of $VOCl_3$ plus additional basis functions from the atoms of the common ligands of complexes **Ia**-**Va** as "ghost basis". The results of these different strategies are summarized in Table 1.

The principal axis directions of the CSA and the EFG tensors are calculated from their eigenvectors and parameterized via the Euler angles. Computations of the Euler angles and drawings of the principal axes of the tensors at the vanadium center were performed with Matlab [55] programs written in our laboratory.

All DFT calculations were executed with Gaussian03 [56] under the Linux environment employing Becke's three-parameter hybrid functional [57, 58] for exchange along with the Lee-Yang-Parr [59] correlation functional (B3LYP). For **Ia**-**Va** extensive calculations of the most important NMR parameters (C_Q,

Table 2. Approximate general error intervals for the NMR parameters Isotropic chemical shift (δ_{iso}), Chemical shift anisotropy (δ_σ), Asymmetry of the CS tensor (η_σ), Quadrupolar coupling constant (C_Q) and Asymmetry of the EFG tensor (η_Q).

δ_{iso} *(ppm)*	δ_σ *(ppm)*	η_σ	C_Q *(MHz)*	η_Q
±0.05	±20	±0.1	±0.2	±0.1

η_Q, δ_{iso}, δ_σ, η_σ, α, β and γ) were performed with Pople's double-ζ and triple-ζ basis sets 6–31G(d), 6–31++G(d, p), 6–311G(d) [60–62] as well as the basis set combination 6–311G(d) opt. 6–311G [30] and with Ahlrichs triple-ζ basis sets TZV and TZVP [63, 64]. To study the influence of the referencing strategy on the δ_{iso} values, calculations with the basis sets 6–311G and 6–311+G were also performed.

3. Experimental section

The *cis*-dioxovanadium(V) complexes **I** and **II** were synthesized starting from the appropriate Schiff-base ligand by reaction with ammonium metavanadate according to procedures similarly described in the literature [44, 46]. The oxovanadium(V) complexes **III** [20], **IV** [47] and **V** [48, 49] were synthesized according to published procedures.

All ^{51}V MAS spectra were measured at two different spinning speeds (7 kHz and 10 kHz) at a resonance frequency of 105.19 MHz corresponding to a field of 9.4 T on a Bruker AMX 400 spectrometer at room temperature [30, 34]. The spectra measured at 10 kHz are displayed in Fig. 2.

The eight NMR parameters (quadrupolar coupling constant C_Q, asymmetry of the EFG tensor η_Q, isotropic chemical shift δ_{iso}, chemical shift anisotropy δ_σ, asymmetry of the CSA tensor η_σ and the Euler angles α, β and γ) were obtained by least-squares fitting of the simulated to the experimental spectrum by a program written in our laboratory. This program is based on a combination of genetic and simplex algorithms and uses the SIMPSON [65] software package as calculational kernel. Details of this program are beyond the scope of this publication and will be published elsewhere.

In principle it is possible to determine exactly the error intervals of each parameter with our method. In practice however this would again imply the cumbersome application of numerically expensive downhill-simplex optimization. Therefore, we estimated the error intervals by comparison of the results of the genetic algorithm on the one hand with the results of the genetic algorithm with subsequent downhill-simplex optimization on the other hand for some complexes. According to our experience, the error values for the parameters obtained by the genetic fitting routine are in the ranges given in Table 2.

The Euler angles, being obtained by our method, must be regarded critically. For the exact determination of the Euler angles, the spectra would have to be fitted by gradient or downhill-simplex fitting methods in addition to the genetic

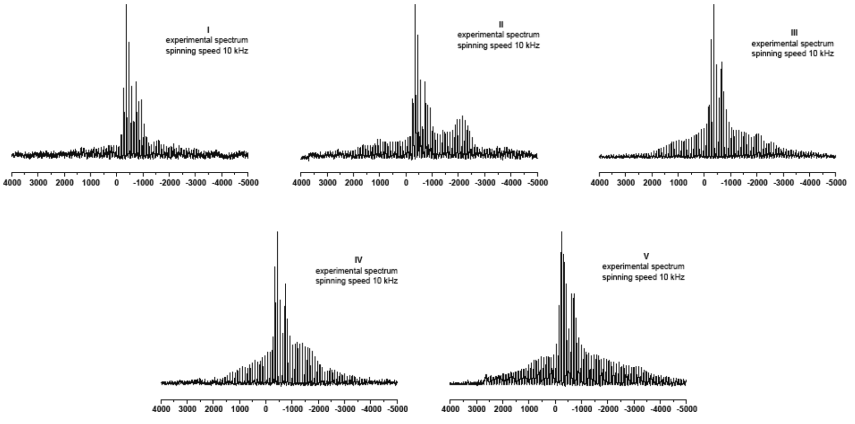

Fig. 2. ^{51}V MAS NMR spectra of the vanadium complexes **I**-**V** acquired at 9.4 T and a spinning speed of 10 kHz. The scale is in ppm, referenced to $VOCl_3$.

fitting routines, due to the fact that genetic algorithms do not reach the minimum exactly [66]. Moreover, the fitting process would have to be performed with a larger number of crystallite orientations. Due to time constraints, both methods are not applicable for the examination of a large number of complexes. In this context, it is worth mentioning, that we performed numerous tests to assure the stability and thus correctness of the other parameters by varying the input parameters and number of integration angles.

We found out, that the number of integration angles does not have a significant influence on the isotropic chemical shift, the chemical shift anisotropy, the quadrupolar coupling constant and the two asymmetry parameters.

4. Results and discussion

4.1 Calculation of isotropic chemical shifts

Figure 3 compares experimental and calculated δ_{iso} values employing Poples double-ζ basis sets 6–31G(d) and 6–31++G(d, p) for the different referencing strategies. The variation of the referencing values of $VOCl_3$ yields no significant improvement of δ_{iso}. With the exception of complex **III**, the calculation with the 6–31G(d) basis and an additional "ghost basis" according to strategy (ii) or (iii) does not improve the referencing value of $VOCl_3$. A similar result is found for the 6–31++G(d, p) basis set. The δ_{iso} values calculated with several referencing values for $VOCl_3$ vary around the experimental δ_{iso} values without any trend.

A rather different behavior of the δ_{iso} values is found if triple-ζ basis sets are used for the computations. Figures 4 and 5 show that the referencing to the

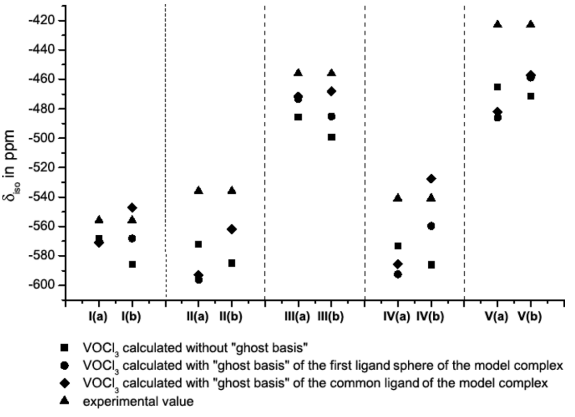

Fig. 3. Comparison between isotropic chemical shift values calculated for complexes **I**-**V** with the 6–31G(d) (a) and the 6–31++G(d,p) (b) basis set using different referencing values for $VOCl_3$ and the experimental values.

absolute shielding values of $VOCl_3$ computed with the "ghost basis" of the atoms of the first coordination spheres of the complexes according to strategy (ii) leads to a significant improvement of the δ_{iso} values in the range of 15–85 ppm. Further improvements are obtained if the absolute shielding values of $VOCl_3$ are calculated with the "ghost basis" of the common ligands of the complexes according to strategy (iii). Nevertheless, there is only a slight difference between the results treated with strategy (ii) and (iii) in the range of 2–20 ppm. Therefore it can be assumed that the atoms of the outer ligand sphere have only a small influence on the vanadium atom. The highest improvement is reached for the triple-ζ basis sets 6–311G, 6–311+G and TZV which contain no polarization functions.

The size of the energy gap between $VOCl_3$ calculated with and without "ghost basis" seems to be one reason for this result. Quantitative relations (Table 3) show that for basis sets without polarization functions like 6–311G, 6–311+G and TZV the energy gap ($\Delta E \approx 45$–125 kJ/mol) is generally larger than for basis sets with additional polarization functions ($\Delta E \approx 20$–80 kJ/mol). The largest energy gaps are calculated with the 6–311G basis set which causes a significant improvement of δ_{iso} in the range of 50–80 ppm for all calculated model complexes. For the TZVP basis set the calculated energy gap is surprisingly very small (20–40 kJ/mol). Accordingly, practically no significant improvements of the δ_{iso} values are achieved, similar to the case of the double-ζ basis sets 6–31G(d) and 6–31++G(d, p) discussed above.

4.2 Quadrupolar coupling and chemical shift anisotropy

Table 4 summarizes the ^{51}V NMR parameters for complexes **I**-**V**, which describe the quadrupolar and chemical shift anisotropy interactions, by comparing the

Table 3. Calculated energy gaps in kJ/mol between $VOCl_3$ calculated without "ghost basis" and with the "ghost basis" of the first ligand sphere (frag) and of the common ligand (comp) of the model complexes **Ia**, **IIIa** and **IVa**.

	Ia		**IIIa**		**IVa**	
basis set	frag	comp	frag	comp	frag	comp
6–31G(d)	38.0	48.3	38.2	54.2	41.1	58.8
6–31++G(d, p)	31.7	38.0	30.7	41.1	34.5	45.9
6–311G	69.1	91.0	73.9	104.2	92.8	124.1
6–311+G	50.9	65.2	47.6	70.9	64.0	84.7
6–311G(d)	46.0	62.2	50.6	71.6	56.2	80.5
TZV	58.2	71.9	52.4	77.1	69.0	90.0
TZVP	23.2	29.5	22.0	32.5	24.5	36.3

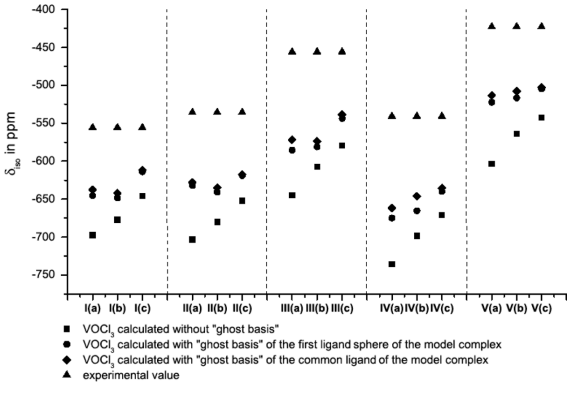

Fig. 4. Comparison between isotropic chemical shift values calculated for complexes **I**-**V** with the 6-311G (a), the 6-311+G (b) and the 6-311G(d) (c) basis sets using different referencing values for $VOCl_3$ and the experimental values.

calculated values employing different sized basis sets with the experimental values.

The quadrupolar coupling constants C_Q for complexes **I**-**V** calculated with the 6–31++G(d,p) using the X-ray model structures **Ia**-**Va** yielded the best agreement with the experimental data (discrepancies smaller than 1 MHz). For the other basis sets, especially Pople's triple-ζ basis sets, the C_Q values are strongly overestimated. Large variations between the C_Q values, treated with different basis sets, are obtained for complexes **I** and **II**. Performing the basis set combination 6–311G(d) opt. 6–311G, which implies that the structure is optimized with the 6–311G basis set and the NMR parameter calculation is done with the 6–311G(d) basis set, the calculated C_Q values are nearly twice as large as the experimental values.

These observations can be understood when looking at the electronic structure of the models. **Ia** and **IIa** are negatively charged. Therefore they can not

Table 4. Comparison of experimental (exp.) and calculated solid-state NMR parameters with different basis sets using the X-ray model structures **Ia**-**Va** for complexes **I**-**V**: Isotropic chemical shift (δ_{iso}), Chemical shift anisotropy (δ_σ), Asymmetry of the CSA tensor (η_σ), Quadrupolar coupling constant (C_Q), Asymmetry of the EFG tensor (η_Q) and the Euler angles (α, β, γ), describing the relative orientation of CSA and EFG tensors. The experimental δ_{iso} values are referenced to neat $VOCl_3$. The calculated δ_{iso} values are referenced to the calculated absolute shielding values of $VOCl_3$ without using a "ghost basis".

complex	basis set	δ_{iso} (*ppm*)	δ_σ (*ppm*)	η_σ	C_Q (*MHz*)[c]	C_Q (*MHz*)[d]	η_Q	α (deg)	β (deg)	γ (deg)
	6–31G(d)	−568	−620	0.14	7.60	7.01	0.49	2	21	105
	6–31++G(d, p)	−586	−616	0.13	6.90	6.37	0.38	1	23	99
	6–311G(d)	−646	−692	0.11	8.98	8.29	0.34	3	25	70
I	6–311G(d) opt. 6311G[a]	−558	−665	0.22	11.25	10.38	0.53	6	18	83
	TZV	−717	−704	0.14	7.47	6.90	0.40	0	25	103
	TZVP	−646	−679	0.13	7.77	7.17	0.45	1	24	105
	exp.[b]	**–552.4**	**–541**	**0.1**	**6.2**		**0.6**	**29**	**73**	**129**
	6–31G(d)	−572	−581	0.14	7.60	7.02	0.55	2	18	101
	6–31++G(d, p)	−585	−575	0.16	6.96	6.42	0.38	2	21	98
	6–311G(d)	−652	−650	0.13	9.32	8.60	0.31	6	24	74
II	6–311G(d) opt. 6311G[a]	−560	−668	0.20	10.66	9.84	0.61	3	16	82
	TZV	−719	−662	0.15	7.66	7.07	0.39	4	24	81
	TZVP	−649	−639	0.14	7.90	7.29	0.45	2	23	80
	exp.[b]	**–535.9**	**–512**	**0.1**	**6.0**		**0.5**	**23**	**50**	**110**
	6–31G(d)	−486	−511	0.15	5.27	4.86	0.66	2	12	130
	6–31++G(d, p)	−499	−504	0.15	4.05	3.74	0.78	2	16	134
	6–311G(d)	−579	−570	0.18	4.61	4.26	0.82	15	15	31
III	6–311G(d) opt. 6311G[a]	−496	−541	0.19	4.52	4.17	0.69	32	24	30
	TZV	−650	−584	0.18	4.03	3.72	0.85	19	14	32
	TZVP	−563	−564	0.19	4.08	3.77	0.81	19	13	33
	exp.[b]	**–458.4**	**–431**	**0.4**	**3.5**		**0.7**	**28**	**52**	**102**
	6–31G(d)	−573	−405	0.10	3.67	3.39	0.52	82	71	66
	6–31++G(d, p)	−586	−392	0.05	3.72	3.43	0.15	4	64	80
	6–311G(d)	−671	−446	0.11	4.17	3.85	0.17	0	55	77
IV	6–311G(d) opt. 6311G[a]	−555	−498	0.15	4.80	4.43	0.51	68	59	76
	TZV	−745	−455	0.06	3.27	3.02	0.04	13	56	52
	TZVP	−656	−445	0.06	3.36	3.10	0.08	5	61	47
	exp.[b]	**–541.3**	**–448**	**0.3**	**3.3**		**0.5**	**53**	**63**	**107**
	6–31G(d)	−465	−394	0.29	7.41	6.84	0.52	89	6	4
	6–31++G(d, p)	−471	−414	0.27	6.54	6.04	0.75	83	7	4
	6–311G(d)	−543	−464	0.28	7.36	6.79	0.88	83	9	1
V	6–311G(d) opt. 6311G[a]	−418	−499	0.25	7.71	7.12	0.86	73	18	27
	TZV	−608	−474	0.28	6.18	5.70	0.86	79	8	3
	TZVP	−520	−455	0.28	6.43	5.85	0.90	71	8	10
	exp.[b]	**–422.6**	**–490**	**0.4**	**6.3**		**0.7**	**49**	**46**	**73**

a) structure optimized with 6–311G followed by "single point" NMR parameter calculation with 6–311G(d)

b) the experimental Euler angles were fitted with rep 30 which yield to relatively unprecise values

c) Quadrupolar coupling constant calculated with $Q = -5.2 \cdot 10^{-30}\ m^2$

d) Quadrupolar coupling constant calculated with $Q = -4.8 \cdot 10^{-30}\ m^2$

adequately model the neutral solid-state structure of complex **I** and **II**. Furthermore, hydrogen bonds which have an influence on the size of C_Q are neglected in these models. Thus the optimization of **Ia** and **IIa** leads to molecular structures which are not comparable with the parameters observed in the solid-state structure.

In contrast to **I** and **II**, the complexes **III**-**V** form neutral compounds which are not able to build up hydrogen bonding networks. Therefore the three neutral model complexes **IIIa**-**Va** describe the solid-state structure in a way which yields a better agreement between the calculated and the experimental C_Q values.

Another aspect which has to be considered when calculating ^{51}V quadrupolar coupling constants by quantum chemical methods is the accuracy, with which the vanadium nuclear quadrupole moment Q itself is known. Since the quadrupolar interaction is directly proportional to the nuclear quadrupole moment, the relative error of the latter causes a systematic error of the calculated quadrupolar coupling constant C_Q.

In the case of ^{51}V the relative error of the nuclear quadrupole moment is rather large. To the best of our knowledge there are two values given for Q which were determined experimentally by (i) atomic-beam magnetic resonance [50] ($Q = [-5.2 \pm 1] \cdot 10^{-30}$ m^2) and (ii) laser-induced resonance-fluorescence spectroscopy [67] ($Q = [-4.3 \pm 0.5] \cdot 10^{-30}$ m^2), which corresponds to approximately ±20% deviation. Alternatively there is also a more recent calculated value of $Q = [-4.8 \pm 0.1] \cdot 10^{-30}$ m^2 given by Hansen [68], which coincides within the error bars with the other values.

To be consistent with the majority of ^{51}V NMR papers, initially the experimental value of $Q = [-5.2 \pm 1] \cdot 10^{-30}$ m^2 was employed for the calculations of the quadrupolar interactions. In a next step the value of $Q = [-4.8 \pm 0.1] \cdot 10^{-30}$ m^2 was also taken to compare the degree of agreement between experimental and theoretical values for C_Q. Figures 6 and 7 compare these theoretical results treated with the two double-ζ basis sets 6–31++G(d, p) and 6–31G(d), respectively the triple-ζ basis set TZV, with the experimental ones. If $Q = [-4.8 \pm 0.1] \cdot 10^{-30}$ m^2 is employed for the calculations of C_Q, especially for complexes **I**, **II** and **III** a significant better agreement between calculated and experimental value is found even for the smaller basis sets with fewer polarization functions like TZV or 6–31G(d) which need smaller computation time to calculate the EFG tensors.

To summarize these results it can be pointed out that according to Hansens results for $AlVO_4$ [68] for our vanadium(V) model complexes a higher degree of consistence between experimental and theoretical value for the quadrupolar coupling constant C_Q is reached if $Q = [-4.8 \pm 0.1] \cdot 10^{-30}$ m^2 is employed in the DFT calculations.

A trend similar to what is found for the C_Q values is also observed for the chemical shift anisotropy values of **I, II** and **III**, for which the calculated δ_σ values are strongly overestimated. For these three complexes the best agreement between calculated and experimental data is found for the 6–31++G(d,p) basis

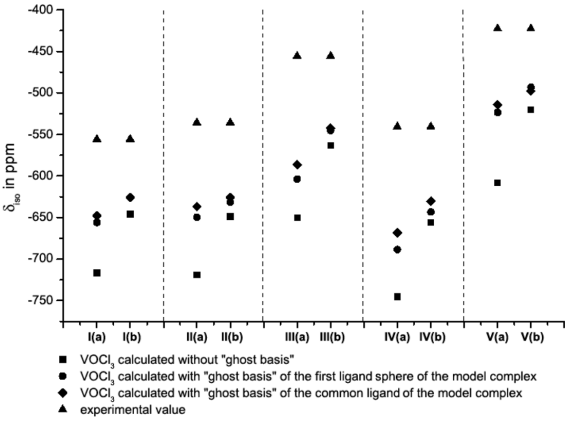

Fig. 5. Comparison between isotropic chemical shift values calculated for complexes **I**-**V** with the TZV (a) and the TZVP (b) basis sets using different referencing values for $VOCl_3$ and the experimental values.

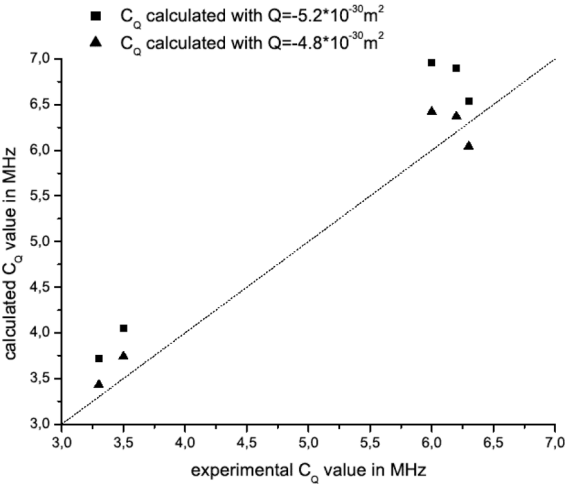

Fig. 6. Correlation between experimental and theoretical *CQ* value calculated with the 6-31++G(d,p) basis set using different values for the quadrupolar moment *Q*.

set. Complexes **IV** and **V** exhibit a different trend of the δ_σ values. While for **IV** good agreement of calculated and experimental values is found for the employed basis sets, the δ_σ values for **V** are underestimated for these basis sets. One possible reason for these results are the structure elements of the ligand spheres including the vanadium center. Whereas **I**-**III** contain large nearly planar

heterocyclic ring systems, **IV** only contains a small planar ring system and **V** contains no planar structure elements at all.

4.3 Absolute orientations of the PAS's of CSA and EFG tensors

Figure 8 displays the directions of the principal axes of the EFG and CSA tensors of the model complexes **Ia**-**Va** calculated with the 6–31++G(d,p) basis set in the molecular frame. In those complexes which include local symmetry elements like planes or rotating axes group theory demands that the orientation of the principal axes of the interaction tensors correlate to these symmetries. This symmetry constraint was also corroborated by DFT calculations of the EFG and CSA tensors of other molecules [29, 68–71]. In complex **Ia** (Fig. 8a) σ_Y and σ_Z form a plane which is located in the nearly planar salicylidene hydrazide ligand system of the complex whereas σ_X is orientated perpendicular to this plane. The largest component V_Z of the EFG is approximately parallel to this σ_Y σ_Z -plane with $\varphi \approx 10^{\circ}$. In complex **IIa** (Fig. 8b) the V_X and the σ_Z axes are located in the planar ligand system. The V_Z and the σ_Z components includes an angle of $\varphi \approx 125^{\circ}$.

Complex **IIIa** (Fig. 8c) which contains two nearly planar ligand systems forming an angle of 77° shows a special arrangement of CSA and EFG tensor. V_Z and V_Y as well as σ_Z and σ_Y form plains which are nearly parallel to the plain of the quinoline ligand with $\theta_{\sigma_Z\sigma_Y} \approx 16^{\circ}$ and $\theta_{V_ZV_Y} \approx 29^{\circ}$. Otherwise V_X and V_Y form a plain which is approximately parallel to the salicylidene hydrazide ligand system with $\theta_{V_XV_Y} \approx 12^{\circ}$. The V_X V_Y -plain also includes the σ_X axis with $\varphi \approx 7^{\circ}$.

Model complexes **IVa** (Fig. 8d) and **Va** (Fig. 8e) contain no special symmetry elements. Surprisingly, in both models the V_Z axis is located in the σ_X σ_Y -plain and therefore the σ_Z axis is arranged in the V_X V_Y -plain. In **IVa** the EFG and CSA tensor are orientated almost perpendicular. The largest components V_Z and σ_Z enclose an angle of $\varphi \approx 71^{\circ}$. Moreover V_X and σ_Y are arranged antiparallel whereas V_X is ranged along the V-O bond of the free oxo-ligand.

5. Conclusion

In this work we calculated ^{51}V solid-state NMR parameters of five different model complexes for vanadium haloperoxidases with DFT methods using the B3LYP functional. The comparison between calculated and experimental values extracted by stepwise fitting of simulated to experimental spectra yields new insights into the problem of practical choice of computational models, basis sets and the referencing system in vanadium NMR. For triple-ζ basis sets, it is shown that the energy gap between $VOCl_3$ calculated with and without "ghost basis" has a significant influence on the calculated absolute shielding value of the referencing standard $VOCl_3$ and therefore on the agreement between calculated and experimental δ_{iso} values of the model complexes. It is found that the quadrupolar

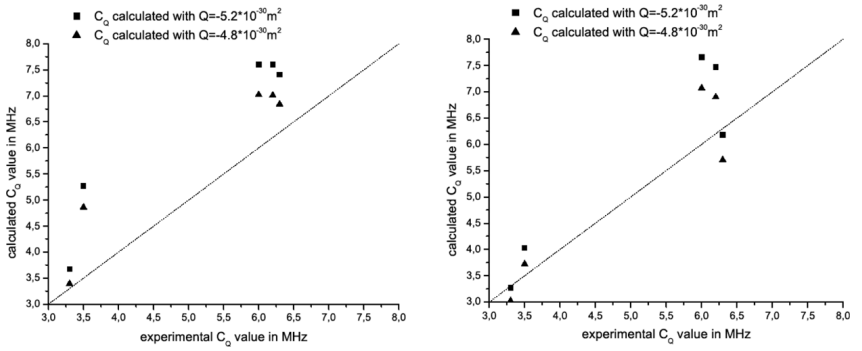

Fig. 7. Correlation between experimental and theoretical C_Q value calculated with the 6-31G(d) basis set (left) and the TZV basis set (right) using different values for the quadrupolar moment Q.

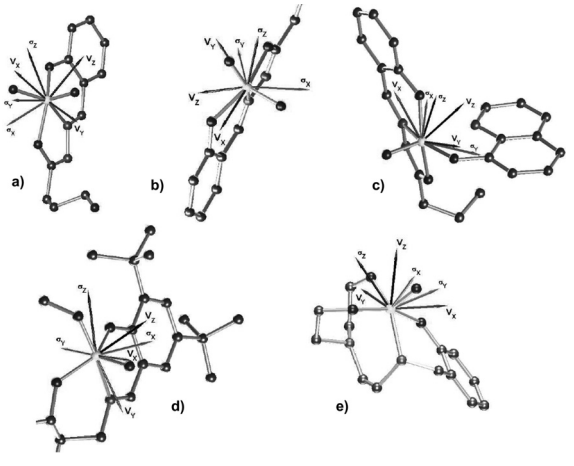

Fig. 8. Absolute orientation of the principal axes of the CSA (σ_X, σ_Y, σ_Z) and the EFG (*VX*, *VY*, *VZ*) tensor in model complexes (a)Ia (b)IIa (c)IIIa (d)IVa (e)Va calculated with the 6-31++G(d,p) basis set.

coupling constant C_Q and the chemical shift anisotropy δ_σ displays the best agreement with the experimental data if basis functions located at atomic positions of the solid-state X-ray structure of the complexes are combined with the 6–31++G(d, p) basis set for the computations. In addition our calculations corroborate the results by Hansen et al. [68], who suggested a new value of $Q = -4.8 \cdot 10^{-30}$ m^2 for the quadrupolar moment of the vanadium nucleus. Finally, correlations between the absolute orientations of the principal axes of CSA and EFG tensors and structure elements of the model complexes could be

established by DFT calculations. In further studies we are investigating the effect of the functional on the calculation of the ^{51}V NMR parameters.

Acknowledgement

We thank the Institute of Organic and Macromolecular Chemistry (IOMC) for supplying their cluster (officer: Dr. Stefan Kluge) and the computing center of the Friedrich-Schiller Universität for supplying their Cray XD1 (officer: Sabine Irmer). Furthermore we thank Dr. Dirk Bender for technical support. Financial support by the Deutsche Forschungsgemeinschaft is gratefully acknowledged.

References

1. H. Manz, Metall und Erz **10** (1913) 379.
2. M. N. Isupov, A. R. Dalby, A. A. Brindley, Y. Izumi, T. Tanabe, G. N. Murshudov, J. A. Littlechild, J. Mol. Biol. **299** (2000) 1035.
3. A. Messerschmidt, R. Wever, Proc. Natl. Acad. Sci. U. S. A. **93** (1996) 392.
4. H. Vilter, Phytochemistry **23** (1984) 1387.
5. M. Weyand, H. J. Hecht, M. Kiess, M. F. Liaud, H. Vilter, D. Schomburg, J. Mol. Biol. **293** (1999) 595.
6. A. Butler, Science **281** (1998) 207.
7. A. Butler, J. N. Carter-Franklin, Nat. Prod. Rep. **21** (2004) 180.
8. G. W. Gribble, Acc. Chem. Res. **31** (1998) 141.
9. R. C. Allen, Biochem. Biophys. Res. Commun. **63** (1975) 675.
10. M. Bangesh, W. Plass, J. Mol. Struct. **725** (2005) 163.
11. Z. Hasan, R. Renirie, R. Kerkman, H. J. Ruijssenaars, A. F. Hartog, R. Wever, J. Biol. Chem. **281** (2006) 9738.
12. J. Y. Kravitz, V. L. Pecoraro, H. A. Carlson, J. Chem. Theory Comput. **1** (2005) 1265.
13. W. Plass, Angew. Chem. Int. Ed. **38** (1999) 909.
14. W. Plass, M. Bangesh, S. Nica, A. Buchholz, ACS Symp. Ser. **974** (2007) 163.
15. E. J. Baran, J. Braz. Chem. Soc. **14** (2003) 878.
16. A. Butler, Coord. Chem. Rev. **187** (1999) 17.
17. D. Rehder, Coord. Chem. Rev. **182** (1999) 297.
18. D. Rehder, Inorg. Chem. Commun. **6** (2003) 604.
19. J. Y. Kravitz, V. L. Pecoraro, Pure Appl. Chem. **77** (2005) 1595.
20. S. Nica, M. Rudolph, H. Görls, W. Plass, Inorg. Chim. Acta **360** (2007) 1743.
21. O. Bortolini, V. Conte, J. Inorg. Biochem. **99** (2005) 1549.
22. D. C. Crans, J. J. Smee, E. Gaidamauskas, L. Q. Yang, Chem. Rev. **104** (2004) 849.
23. J. Hartung, Pure Appl. Chem. **77** (2005) 1559.
24. I. Lippold, H. Görls, W. Plass, Eur. J. Inorg. Chem. (2007) 1487.
25. B. A. Gee, A. Wong, J. Phys. Chem. B **107** (2003) 8382.
26. U. G. Nielsen, A. Boisen, M. Brorson, C. J. H. Jacobsen, H. J. Jakobsen, J. Skibsted, Inorg. Chem. **41** (2002) 6432.
27. U. G. Nielsen, H. J. Jakobsen, J. Skibsted, J. Phys. Chem. B **105** (2001) 420.
28. U. G. Nielsen, N. Y. Topsoe, M. Brorson, J. Skibsted, H. J. Jakobsen, J. Am. Chem. Soc. **126** (2004) 4926.
29. N. Pooransingh, E. Pomerantseva, M. Ebel, S. Jantzen, D. Rehder, T. Polenova, Inorg. Chem. **42** (2003) 1256.
30. A. Schweitzer, T. Gutmann, M. Wächtler, H. Breitzke, A. Buchholz, W. Plass, G. Buntkowsky, Solid State NMR (2008) doi: 10.1016 / j.ssnmr.2008.02.003.

31. J. Skibsted, C. J. H. Jacobsen, H. J. Jakobsen, Inorg. Chem. **37** (1998) 3083.
32. J. Skibsted, N. C. Nielsen, H. Bildsoe, H. J. Jakobsen, Chem. Phys. Lett. **188** (1992) 405.
33. J. Skibsted, N. C. Nielsen, H. Bildsoe, H. J. Jakobsen, J. Am. Chem. Soc. **115** (1993) 7351.
34. S. Nica, A. Buchholz, M. Rudolph, A. Schweitzer, M. Wächtler, H. Breitzke, G. Buntkowsky, W. Plass, Eur. J. Inorg. Chem. (2008) 2350.
35. G. Buntkowsky, W. Hoffmann, T. Kupka, G. Pasternad, M. Jaworska, H. M. Vieth, J. Phys. Chem. A **102** (1998) 5794.
36. G. Buntkowsky, I. Sack, H.-H. Limbach, B. Kling, J. Fuhrhop, J. Phys. Chem. B **101** (1997) 11265.
37. S. Macholl, F. Boerner, G. Buntkowsky, Chem. Eur. J. **10** (2004) 4808
38. S. Macholl, D. Lentz, F. Borner, G. Buntkowsky, Chem. Eur. J. **13** (2007) 6139.
39. N. Pooransingh-Margolis, R. Renirie, Z. Hasan, R. Wever, A. J. Vega, T. Polenova, J. Am. Chem. Soc. **128** (2006) 5190.
40. M. P. Waller, M. Bühl, K. R. Geethalakshmi, D. Wang, W. Thiel, Chem. Eur. J. **13** (2007) 4723.
41. K. J. Ooms, S. E. Bolte, J. J. Smee, B. Baruah, D. C. Crans, T. Polenova, Inorg. Chem. **46** (2007) 9285.
42. S. Macholl, F. Börner, G. Buntkowsky, Z. Phys. Chem. **217** (2003) 1483.
43. S. F. Boys, F. Bernardi, Mol. Phys. **19** (1970) 553.
44. S. Nica, A. Pohlmann, W. Plass, Eur. J. Inorg. Chem. (2005) 2032.
45. W. Plass, Coord. Chem. Rev. **237** (2003) 205.
46. A. Pohlmann, S. Nica, T. K. K. Luong, W. Plass, Inorg. Chem. Commun. **8** (2005) 289.
47. I. Lippold, J. Becher, D. Klemm, W. Plass, J. Mol. Catal. A: Chemical (2008), submitted.
48. W. Plass, Inorg. Chim. Acta **244** (1996) 221.
49. W. Plass, Z. Anorg. Allg. Chem. **623** (1997) 461.
50. W. J. Childs, Phys. Rev. **156** (1967) 71.
51. M. E. Smith, E. R. H. van Eck, Prog. Nucl. Magn. Reson. Spectrosc. **34** (1999) 159.
52. M. E. Rose, *Elementary Theory of Angular Momentum.* Wiley: New York (1957).
53. C. Fernandez, P. Bodart, J. P. Amoureux, Solid State NMR **3** (1994) 79.
54. S. I. Troyanov, Russ. J. Inorg. Chem. **50** (2005) 1727.
55. Matlab; R2007A ed.
56. M. J. Frisch, G. W. Trucks, H. B. Schlegel, G. E. Scuseria, M. A. Robb, J. R. Cheeseman, J. Montgomery, T. J. A.; Vreven, K. N. Kudin, J. C. Burant, J. M. Millam, S. S. Iyengar, J. Tomasi, V. Barone, B. Mennucci, M. Cossi, G. Scalmani, N. Rega, G. A. Petersson, H. Nakatsuji, M. Hada, M. Ehara, K. Toyota, R. Fukuda, J. Hasegawa, M. Ishida, T. Nakajima, Y. Honda, O. Kitao, H. Nakai, M. Klene, X. Li, J. E. Knox, H. P. Hratchian, J. B. Cross, V. Bakken, C. Adamo, J. Jaramillo, R. Gomperts, R. E. Stratmann, O. Yazyev, A. J. Austin, R. Cammi, C. Pomelli, J. W. Ochterski, P. Y. Ayala, K. Morokuma, G. A. Voth, P. Salvador, J. J. Dannenberg, V. G. Zakrzewski, S. Dapprich, A. D. Daniels, M. C. Strain, O. Farkas, D. K. Malick, A. D. Rabuck, K. Raghavachari, J. B. Foresman, J. V. Ortiz, Q. Cui, A. G. Baboul, S. Clifford, J. Cioslowski, B. B. Stefanov, G. Liu, A. Liashenko, P. Piskorz, I. Komaromi, R. L. Martin, D. J. Fox, T. Keith, M. A. Al-Laham, C. Y. Peng, A. Nanayakkara, M. Challacombe, P. M. W. Gill, B. Johnson, W. Chen, M. W. Wong, C.; J. A. Pople, Gaussian 03; Revision C.02 ed.; Gaussian Inc.: Wallingford CT (2004).
57. A. D. Becke, J. Chem. Phys. **98** (1993) 1372.
58. A. D. Becke, J. Chem. Phys. **98** (1993) 5648.
59. C. T. Lee, W. T. Yang, R. G. Parr, Phys. Rev. B **37** (1988) 785.

60. T. Clark, J. Chandrasekhar, G. W. Spitznagel, P. V. Schleyer, J. Comput. Chem. **4** (1983) 294.
61. C. Harihara, J. A. Pople, Theor. Chim. Acta **28** (1973) 213.
62. W. J. Hehre, R. Ditchfield, J. A. Pople, J. Chem. Phys. **56** (1972) 2257.
63. A. Schäfer, H. Horn, R. Ahlrichs, J. Chem. Phys. **97** (1992) 2571.
64. A. Schäfer, C. Huber, R. Ahlrichs, J. Chem. Phys. **100** (1994) 5829.
65. M. Bak, J. T. Rasmussen, N. C. Nielsen, J. Magn. Reson. **147** (2000) 296.
66. D. G. Ireland, S. Janssen, J. Ryckebusch, Nuclear Physics A **740** (2004) 147.
67. P. Unkel, P. Buch, J. Dembczynski, W. Ertmer, U. Johann, Z. Phys. D - Atoms Molecules and Clusters **11** (1989) 259.
68. M. R. Hansen, G. K. H. Madsen, H. J. Jakobsen, J. Skibsted, J. Phys. Chem. B **110** (2006) 5975.
69. D. L. Bryce, K. Eichele, R. E. Wasylishen, Inorg. Chem. **42** (2003) 5085.
70. D. L. Bryce, R. E. Wasylishen, Phys. Chem. Chem. Phys. **4** (2002) 3591.
71. A. Wong, R. Ida, X. Mo, Z. H. Gan, J. Poh, G. Wu, J. Phys. Chem. A **110** (2006) 10084.